

## THERMODYNAMIC AND KINETICS ANALYSIS OF THE SULFUR-FIXED ROASTING OF ANTIMONY SULFIDE USING ZnO AS SULFUR-FIXING AGENT

Z. Ouyang<sup>a</sup>, Y.F. Chen<sup>a</sup>, S.Y. Tian<sup>a</sup>, L. Xiao<sup>a</sup>, C.B. Tang<sup>b</sup>, Y. J. Hu<sup>a</sup>, Z. M. Xia<sup>a</sup>, Y.M. Chen<sup>b</sup>, L.G. Ye<sup>a,\*</sup>

<sup>a</sup>College of Metallurgy and Material Engineering, Hunan University of Technology, Zhuzhou, China.

<sup>b</sup>School of Metallurgy and Environment, Central South University, Changsha, China.

(Received 10 May 2018; accepted 20 November 2018)

### Abstract

Currently, the commercial antimony metallurgy is mainly based on pyrometallurgical processes and oxidative volatilization of  $Sb_2S_3$  is an essential step. This step includes the problems of high energy consumption and low concentration of  $SO_2$  pollution. Aiming at these problems, we present a new method of sulfur-fixing roasting of antimony sulfide. This method uses ZnO as a sulfur-fixing agent, and roasting with  $Sb_2S_3$  was carried out at 673 K–1073 K to produce  $Sb_2O_3$  and ZnS. By calculating the thermodynamics of the reactions, we can conclude that the Gibbs Free Energy Change ( $\Delta G^\theta$ ) of roasting reaction is below -60 kJ/mol and the predominance areas of  $Sb_2O_3$  and ZnS are wide and right shifting with the temperature increase, which all indicates that this method is theoretically feasible. The reacted products between  $Sb_2S_3$  and ZnO indicated that the reaction began at 773 K and finished approximately at 973K. We used the Ozawa-Flynn-Wall, Kissinger and Coats-Redfern method to calculate the kinetics of the roasting reaction. The conclusion is as follows: The average values of apparent activation energy ( $E$ ) and natural logarithmic frequency factor ( $\ln A$ ) calculated by Ozawa-Flynn-Wall, Kissinger and Coats-Redfern were 189.72 kJ·mol<sup>-1</sup> and 35.29 s<sup>-1</sup>, respectively. The mechanism of this reaction was phase boundary reaction model. The kinetic equation is shown as follow, where  $\alpha$  represents reaction fraction:

$$1-(1-\alpha)^{1/3} = 2.12 \times 10^{15} \exp\left(-\frac{1.90 \times 10^5}{RT}\right) t$$

**Keywords:** Antimony sulfide; Zinc oxide; Sulfur-fixing; Kinetics; Roasting.

### 1. Introduction

Antimony is mainly used in the production of flame retardants and the manufacture of battery materials, sliding bearings ammunition and solders [1]. Most of the resources of antimony known in the world are distributed in China, accounting for 80% [1-2]. At present, the main mineral for producing antimony is stibnite ( $Sb_2S_3$ ) and jamesonite ( $Pb_4FeSb_6S_{14}$ ) [3-5]. The traditional method for the production of antimony is volatilization smelting followed by reduction smelting [6-7], which consists of two steps: oxidative volatilization of  $Sb_2S_3$  and reducing smelting of  $Sb_2O_3$  [8-9]. The reduction smelting is relatively mature and the main equipment is reverberatory furnace with soda addition. However, the oxidative volatilization of  $Sb_2S_3$  is the key process and a large numbers of studies were carried out. At present, the main equipment is blast furnace in practice using air or oxygen-enriched air to oxidize  $Sb_2S_3$  and then generate  $Sb_2O_3$  and  $SO_2$ . The characteristics of this method are thin material layer, high coke rate, and high temperature of furnace roof (>1273K). The disadvantages are high energy

consumption and low concentration  $SO_2$  smoke pollution (<6%). Meanwhile, arsenic, a drug substance associated with  $Sb_2S_3$  ore, is also volatile at high temperature causing environment hazardous.

Hydrometallurgical process, including the acidity and alkaline methods and consisting of a two steps of leaching and electrodeposition, can be used for both simple and complex antimony ore. In practice, NaOH- $Na_2S$  [10] and  $FeCl_3/SbCl_5-HCl$  [11] were the main leaching reagents, direct electrowinning, membrane electrowinning and slurry electrolysis method were the subsequent process of Sb extraction. Samuel a. Awe [12-13] investigated recovering metallic antimony from the copper and sulfur concentrate containing antimony by selective leaching in alkaline sulphide solution. Yang [14] investigated separation and recovery of Sb from stibnite using  $SbCl_5-HCl$  as a leaching reagent and it was regenerated by electrowinning. These methods eliminate the atmospheric pollution caused by  $SO_2$ . However, the shortcomings are the discharge of a large amount of wastewater, equipment corrosion and low current efficiency. Only a few plants applied it to produce antimony white products.

\*Corresponding author: yelonggang@sina.cn



In the area of pyrometallurgy, Liu [15] investigated the bath smelting process of stibnite by using bottom blow furnace and fuming furnace. The advantages are a high volatilization rate of Sb and the elimination of the briquetting process. Hua [16] studied the selective oxidation of antimony sulphide by water vapor. The maximum direct recovery rate of lead and antimony were 97% and 85%. These new methods have improved the traditional process and strengthened the environmental protection. However, the main shortcomings are flue bonding by antimony oxide and valuable metal dispersion at high temperature (>1373K). Generally, these methods have enhanced antimony metallurgy, but there are all far away from industrial manufacture.

Aiming at the problems of SO<sub>2</sub> pollution and the difficulty of Sb<sub>2</sub>O<sub>3</sub> production at high temperature, R. Padilla [17] adopted the direct reduction of metal sulfides in the presence of lime. In this method, lime and carbon were used as the sulfur-fixing agent and reductant, respectively, and metallic Sb and CaS were the final products. This method solved the problem of SO<sub>2</sub> pollution and realized the direct produce of Sb. However, this method consumed a large amount of lime and generated large amounts of calcium sulfide slag, which is not easy to be separated and utilized again. Our team [18] once proposed a one-step process to extract antimony from low-grade stibnite in Na<sub>2</sub>CO<sub>3</sub>-NaCl binary molten salt at a low temperature (873-1173K). However, the regeneration of molten salt was difficult.

In view of the above issues, we proposed a sulfur-fixing and low temperature roasting process to produce Sb<sub>2</sub>O<sub>3</sub> using a reproducible and available sulfur-fixing agent to replace lime, and Sb<sub>2</sub>O<sub>3</sub> can be volatilized for separation from roasted products, or the sulfide can be separated by flotation. Then the Sb<sub>2</sub>O<sub>3</sub> can be engaged in the reducing process by the current reverberatory furnace process. Meanwhile, a large amount of zinc oxide (ZnO) ash was produced in lead and zinc smelter [19-20], and its main component was ZnO (>70%) while contained fluorine (>0.2%) and chlorine (>0.3%). If it is directly returned to the hydrometallurgy of zinc, it will cause the plate corrosion. Therefore, it needs to be defluorinated and dechlorinated at high temperature (>1273K), causing a high energy consumption. Hence, we assumed that the ZnO ash can be used for sulfur-fixing of Sb<sub>2</sub>S<sub>3</sub> and converted to ZnS at low temperature (673K-1073K). Then ZnS can be separated by conventional flotation to obtain zinc concentrate [21-22], and it can be utilized as a raw material for Zn metallurgy. This method has the advantages of eliminating the SO<sub>2</sub> emission, removing of fluorine and chlorine, and the low energy consumption since the low temperature roasting process between ZnO and Sb<sub>2</sub>S<sub>3</sub> might be solid-solid or solid-liquid reaction, and the kinetic

speed has a practical significance. Therefore, this work investigated the thermodynamics and kinetics of the roasting reaction, and this method may have a potential application for the production of the congeneric sulfide ore and comprehensive oxide ash utilization.

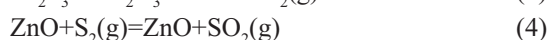
## 2. Experimental

### 2.1. Experimental agents and instruments

The raw materials included zinc oxide (ZnO, Sinopharm Co. Ltd. PRC) and antimony sulfide (Sb<sub>2</sub>S<sub>3</sub>, WengJiang Reagent Co. Ltd. PRC) used for roasting experiments are all analytical grade. The roasting reactions were conducted in a tubular furnace (SGM, T60/12A, Sigma Furnace Co. Ltd. PRC). The thermogravimetric and differential scanning calorimetry instrument (TG-DSC, Universal V4.0C TA Instrument, USA) was used for the detection of thermal effects and weight changes between the reaction of ZnO and Sb<sub>2</sub>S<sub>3</sub>. The uniform mixture of ZnO Sb<sub>2</sub>S<sub>3</sub> was prepared by solution dispersion using an ultrasonic machine (KQ5200DA, KunShan Ultrasonic Instrument Co. Ltd. PRC). The phase and morphology of the products were detected by X ray diffractometer (XRD, Rigaku D/max 2550VB + 18 kW) and scanning electron microscopy (JSM-6490LV, JEOL).

### 2.2. The experimental procedure

The uniform mixture of Sb<sub>2</sub>S<sub>3</sub> and ZnO was prepared by the following steps: (i) A total of 35 g of antimony sulfide and zinc oxide powder, both with the particle of 250-300 mesh, were weighed according to the mole ratio of equation (1); (ii) The mixture powder was pulpified by 75ml of alcohol with a mechanical mixer for 30min in the ultrasonic machine; (iii) The seriflux was dried in the blast oven at 323K, and the final drying mixture was sealed and kept in a dryer and used as a raw material for all experiments. In the roasting experiments, each 5g of the sample was pressed to a block cylinder (Ø1cm) at 12 MPa, and then it was charged in a crucible and located in the hot zone of the tube furnace in the temperature range of 673K to 1173K at argon atmosphere. After the predetermined reaction time, the crucible was quickly pushed out of the hot zone and quenched to room temperature at argon. The reactions that might occur during the roasting process are as follows [23-24]:



After cooling sufficiently, the roasting products



were grounded to fine particles for XRD and SEM detection. TG-DSC experiments, used for kinetics calculations, were carried out in nitrogen atmosphere at a flow of 100 mL/min with different heating rate of 5 K/min to 20 K/min. The kinetics equations were calculated by Ozawa-Flynn-Wall, Kissinger and Coats-Redfern methods by the following formulas [25-26]:

$$\text{Mass action law: } \frac{d\alpha}{dt} = kf(\alpha) \quad (4)$$

$$\text{Arrhenius formula: } k = A \exp\left(-\frac{E}{RT}\right) \quad (5)$$

$$\text{Ozawa-Flynn-Wall method: } \log\beta = \log \frac{AE}{Rf(\alpha)} - 2.315 - 0.4567 \frac{E}{RT} \quad (6)$$

$$\text{Kissinger method: } \ln \frac{\beta}{T_p^2} = \ln \frac{AR}{E} - \frac{E}{R T_p} \quad (7)$$

$$\text{Coats-Redfern method: } \ln \left[ \frac{G(\alpha)}{T^2} \right] = \ln \left[ \frac{AR}{\beta E} \right] - \frac{E}{RT} \quad (8)$$

where  $\alpha$  is reaction fraction, %;  $t$  is reaction time, s;  $k$  is reaction rate constant, s<sup>-1</sup>;  $A$  is frequency factor, s<sup>-1</sup>;  $E$  is active energy, kJ/mol;  $R$  is gas constant 8.314, J/mol·K;  $T$  is temperature, K;  $\beta$  the heating rate, K/min;  $n$  is reaction order number;  $T_p$  the peak temperature, K;  $f(\alpha)$  and  $G(\alpha)$  are integral expressions depended on the particular decomposition mechanism of solid reaction listed in Table 1 [27-29].

**Table 1.** Reaction models and the corresponding functions of the solid reaction

Symbol of reaction models	Reaction models	G(α)	f(α)
P <sub>2</sub>	Power law	α <sup>1/2</sup>	2α <sup>1/2</sup>
P <sub>3</sub>	Power law	α <sup>1/3</sup>	3α <sup>2/3</sup>
P <sub>4</sub>	Power law	α <sup>1/4</sup>	α <sup>3/4</sup>
R <sub>1</sub>	Phase boundary reaction	α	1
R <sub>2</sub>	Phase boundary reaction	1-(1-α) <sup>1/2</sup>	2(1-α) <sup>1/2</sup>
R <sub>3</sub>	Phase boundary reaction	1-(1-α) <sup>1/3</sup>	3(1-α) <sup>2/3</sup>
D <sub>1</sub>	One-dimensional diffusion	α <sup>2</sup>	α <sup>-1/2</sup>
D <sub>2</sub>	Two-dimensional diffusion	α+(1-α)ln(1-α)	[-ln(1-α)] <sup>-1</sup>
A <sub>n</sub>	Avrami-Erofeev (n=1.5,2,3,4)	[-ln(1-α)] <sup>1/n</sup>	n(1-α)[-ln(1-α)] <sup>-(1/n-1)</sup>

### 3. Results and Discussion

#### 3.1. Thermodynamics analysis

To investigate the feasibility of the roasting reactions, HSC software was used to calculate the predominance area and thermodynamic equilibrium of the Sb<sub>2</sub>S<sub>3</sub> - ZnO system, the results are shown in Fig.1. It can be seen from the Fig.1(a) that the objective areas of predominance were in equilibrium with the vapor phase at 773 K, 973 K and 1173 K, and the stable regions of Sb<sub>2</sub>O<sub>3</sub> and ZnS were presented with a wide concentration range of O<sub>2</sub> partial pressure (P<sub>O2</sub>) 10<sup>-12</sup> to 10<sup>-18</sup> and sulfur partial pressure (P<sub>S2</sub>) 10<sup>-1.5</sup> to 10<sup>-8.3</sup> in the gas phase. Meanwhile, the equilibrium area of antimony oxide and zinc sulfide was gradually moving to the upper and right axis with the temperature increase. It shows that the P<sub>O2</sub> and P<sub>S2</sub> increased, so the equilibrium required conditions are easier to achieve. However, if the reaction equilibrium was conducted at a high partial pressure of gaseous sulfur, oxygen and temperature, then antimony sulfate would be yield and it was adverse for Sb<sub>2</sub>O<sub>3</sub> generation and reducing. Therefore, a relative oxygen-free or reducing atmosphere was needed, as well as a low roasting temperature. Fig. 1(b) shows

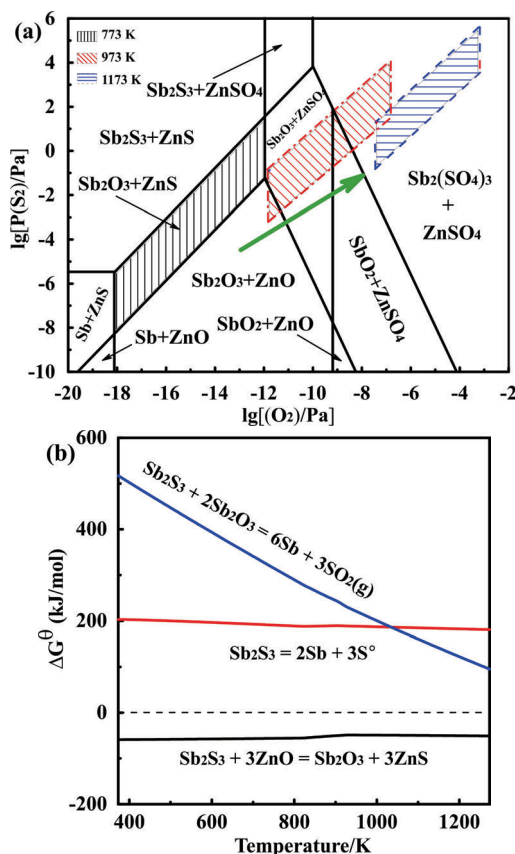


**Figure 1.** The equilibrium dominance zone (a) and thermodynamic equilibrium curve (b) of the Sb-S-O system



that the  $\Delta G^0$  of the reaction (1) is negative in the temperature range of 373 K to 1273 K, which indicated that the interaction between zinc oxide and antimony sulfide is a feasibility in thermodynamics. For reaction (2) and reaction (3), the  $\Delta G^0$  values are both positive between 373 K and 1273 K, so they are not spontaneous in theory. But the  $\Delta G^0$  value of equation (3) decreased quickly with the temperature increase and it might occur at high temperatures.

### 3.2. Procedure analysis

The TG-DSC curves of the reaction between  $Sb_2S_3$  and ZnO with a heating rate of  $10\text{ K}\cdot\text{min}^{-1}$  is presented in Fig.2(a). As shown in DSC curve, there was an exothermic peak at 782.47 K and an endothermic peak at 901.63 K. According to the TG curve, we can see that the reaction has two stages of weight losses. The losses rate of the weight for the first stage is 2.36%, which was caused by the volatilization of the raw mixture at the exothermic peak of 782.47 K. In the second stage, the weight losses rate was 15.78% might cause by the volatilization of  $Sb_2O_3$  and  $Sb_2S_3$  at 901.63 K, which is close to the melting-point of antimony oxide of 929.15 K. Meanwhile, R. Padilla once investigated the volatilization of antimony sulfide and verified that it would thoroughly volatilize at the temperature ranges of 873 K to 1073 K [4], so this 20% weight loss of mixture is impossible by volatilization of  $Sb_2S_3$ . In order to find out the phase composition of the product in two weightlessness stages, the XRD patterns of the samples obtained at different temperatures are shown in Fig.2(b).

The roasted products at 673 K were basically antimony sulfide and zinc oxide, which showed that no reaction occurred. When temperature increased

to 773 K, the peaks of  $Sb_2S_3$  and ZnO still existed while the peaks of  $Sb_2O_3$  and ZnS appeared. It showed that the roasting reactions proceeded, but not completely. With the temperature further increased to 873 K, the peaks of  $Sb_2S_3$  and ZnO gradually disappeared, and only ZnS and  $Sb_2O_3$  left. However, the peak intensity of  $Sb_2O_3$  was gradually decreased. It is found that the vapor pressure of  $Sb_2O_3$  is 2.72 kPa and 6.13 kPa at 973 K and 1073 K, and increases quickly with the temperature increase [30]. So, rapid weight at the second stages in TG curves are caused by the volatilization of  $Sb_2O_3$ . Based on the XRD results, it can be supported that the first exothermic peak at 782.47 K can be attributed to the interaction between  $Sb_2S_3$  and ZnO, and the second endothermic peak was the fusion of  $Sb_2O_3$ .

As shown in Fig.3, images and EDX spectra of the roasting products obtained at 873 K and 1073 K were also studied. It can be seen from the Fig.3 that antimony oxide and zinc sulfide appeared in the sample at 873 K and 1073 K, and it can be inferred that the reaction was more sufficient for a simple images composition at 1073 K. The ZnS was random distributed in  $Sb_2O_3$  particle, and the shape of zinc sulfide is regular polygon. In addition, with increasing the temperature, the  $Sb_2O_3$  particles were getting bigger because it melted at 1073 K and gathered together. However, Fig.3(b) also indicated that little metallic Sb was generated at 1073 K, combined with the thermodynamic calculation, it can be explained by the fact of interaction between  $Sb_2O_3$  and  $Sb_2S_3$ . Reaction smelting, which is the cross reaction between  $Sb_2S_3$  and  $Sb_2O_3$ , was once application in practice for the Sb production according to the reaction (3).

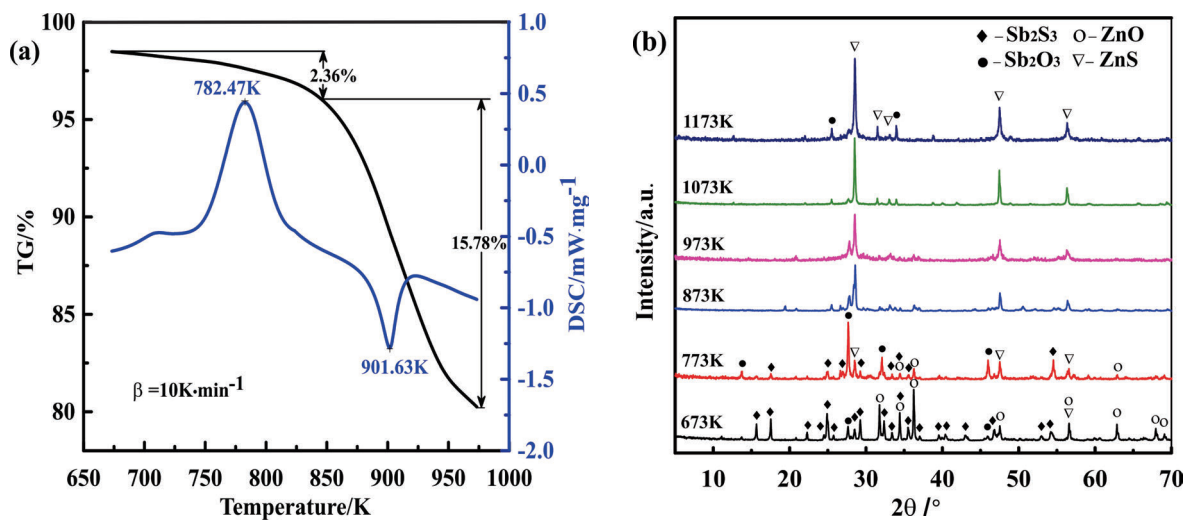


Figure 2. The TG-DSC curves of the reaction between  $Sb_2S_3$  and ZnO at the heating rate of  $10\text{ K}\cdot\text{min}^{-1}$  (a) and the XRD results of the reaction products (b)

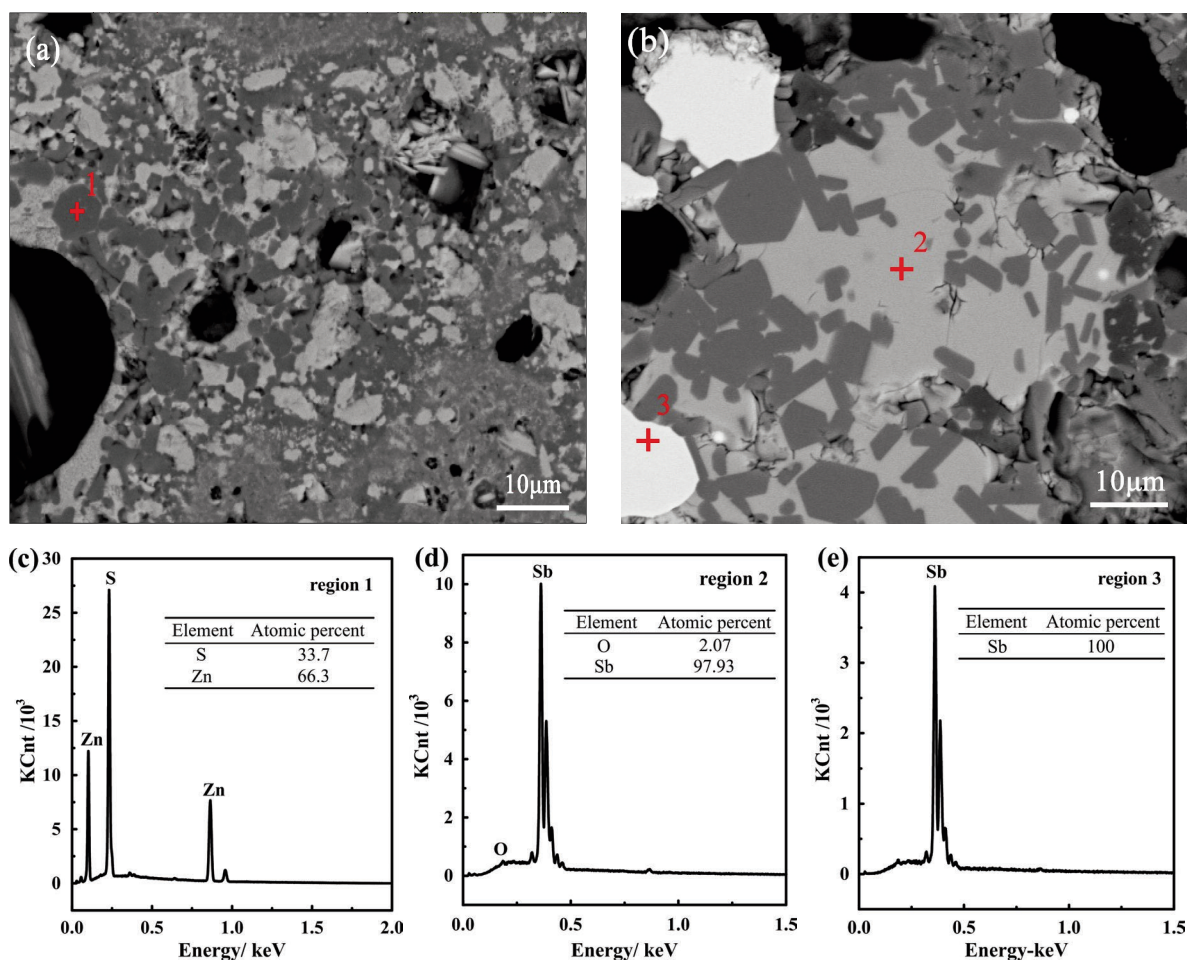


Figure 3. The SEM images of the reaction products at 873K (a) and 1073K (b) and Energy spectrum diagrams of different region

### 3.3. Kinetics analysis

The kinetics of roasting reactions was studied by DSC to obtain kinetic equation including the activation energy and reaction order. In general, three methods including Ozawa-Flynn-Wall, Kissinger and Coats-Redfern method are used for calculating the kinetics parameters. The results of DSC curves of the reaction between  $Sb_2S_3$  and ZnO at different heating rate are shown in Fig.4. From this figure, it can be seen that all four DSC curves have the similar tendency and shape at the heating rates of 10 K/min, 15 K/min, and 20 K/min. However, the thermal effect at 5 K/min was gentle and the peak height was smaller. With the increase in temperature, the position of the peak gradually shifts to right. Based on the above issues, the first peak is the reaction peak of  $Sb_2S_3$  and ZnO, and the second is the melting peak of  $Sb_2O_3$ . The relationship between the conversion rate and the heating temperature can be obtained by integrating the first peak, as shown in Fig.5. According to Fig.5, the reaction kinetics of  $Sb_2S_3$  and

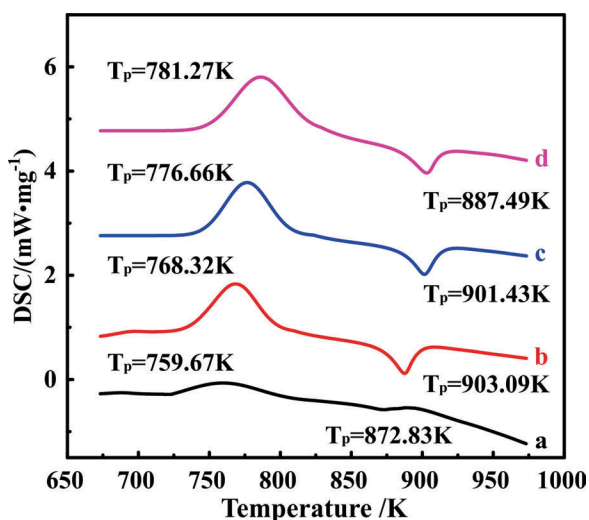


Figure 4. DSC curves of  $Sb_2S_3$ -ZnO mixture reacted at different heating rates (a - 5 K/min, b - 10 K/min, c - 15 K/min, d - 20 K/min)

ZnO were calculated by Ozawa-Flynn-Wall method, Kissinger method and Coats-Redfern method.

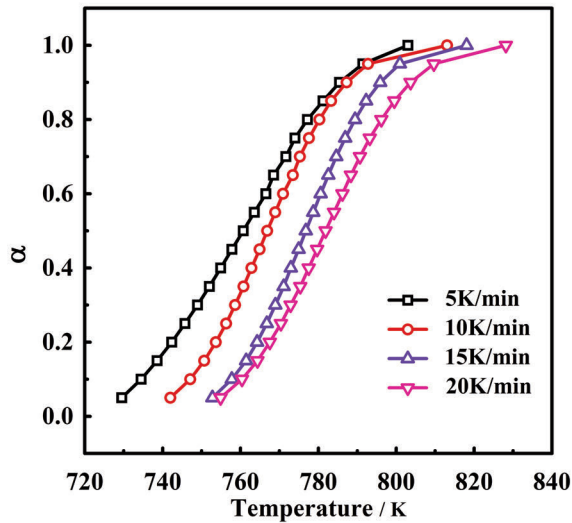


Figure 5. The relationships between reaction fraction and reaction temperature

As shown in Fig.6, the relationships between  $\lg\beta$  and  $1/T$  were calculated by Ozawa-Flynn-Wall method. The data of the slopes, activation energy, correlation coefficients ( $R^2$ ) and residual standard deviation ( $S$ ) calculated from Fig.6 are exhibited in Table 2. It is apparent that when  $\alpha$  increased from 10% to 100%, the  $E$  was corresponding changed from 287.7  $\text{kJ}\cdot\text{mol}^{-1}$  to 310.1  $\text{kJ}\cdot\text{mol}^{-1}$ . The average of the  $E$  is 297.0  $\text{kJ}\cdot\text{mol}^{-1}$ .

The relationships between  $\ln(\beta T_p^{-2})$  and  $1/T_p$  were also calculated by the Kissinger method, and the

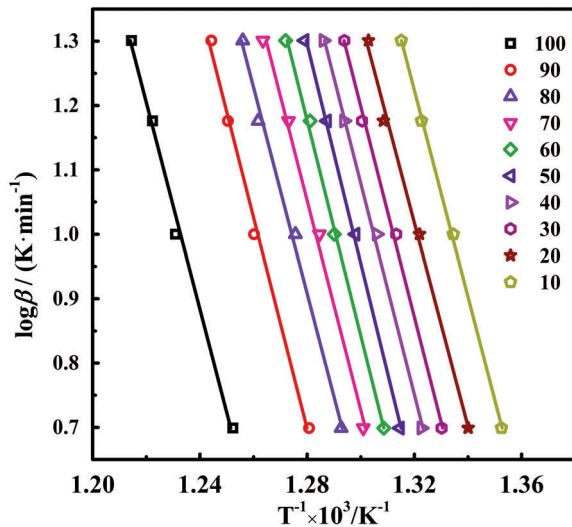


Figure 6. The relationships between  $\lg\beta$   $1/T$  via Ozawa-Flynn-Wall method

results are shown in Fig.7. The corresponding kinetics parameters were exhibited in Table 3. It can be seen that the  $E$  and  $S$  of the roasting reaction are 296.87  $\text{kJ}\cdot\text{mol}^{-1}$  and 38.97  $\text{s}^{-1}$ . Compared with the calculating results by Ozawa-Flynn-Wall method listed in Table 3, it can be found that the calculation results obtained by these two methods were very close.

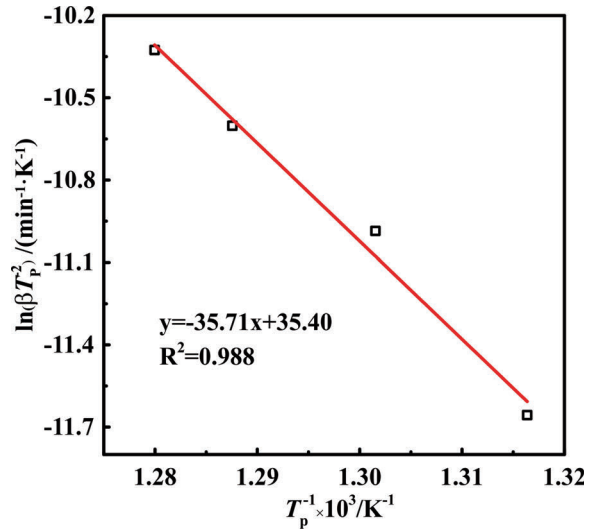


Figure 7. The relationship between  $\ln(\beta T_p^{-2})$  and  $1/T_p$  calculated by Kissinger equation

Table 2. The data of the slopes,  $E$ ,  $S$  and  $R^2$  calculated by Ozawa-Flynn-Wall method

$\alpha$	Slope	$E$ ( $\text{kJ}\cdot\text{mol}^{-1}$ )	$S$	$R^2$
10	-16.03	287.7	$4.65 \times 10^{-7}$	0.996
20	-15.82	288	$3.58 \times 10^{-6}$	0.977
30	-16.37	297.9	$2.14 \times 10^{-6}$	0.997
40	-16.42	298.9	$1.79 \times 10^{-6}$	0.997
50	-17.04	310.1	$1.26 \times 10^{-6}$	0.998
60	-16.72	304.4	$1.63 \times 10^{-6}$	0.997
70	-16.26	296	$4.41 \times 10^{-6}$	0.994
80	-16.03	291.7	$4.55 \times 10^{-6}$	0.994
90	-16.42	298.9	$3.75 \times 10^{-6}$	0.995
100	-16.05	292.2	$4.75 \times 10^{-6}$	0.994
Average		297		

The values of the frequency factor and the activation energy were obtained by the Ozawa-Flynn-Wall and Kissinger methods. In order to obtain the more accurate and reliable date, the Coats-Redfern method was used to calculate the reaction model and its results were shown in Table 4. Based on the data in Table 4 and the results of Ozawa-Flynn-Wall and



**Table 3.** The kinetics parameters conducted by Kissinger equation

Content	Slope	Intercept	E (kJ·mol <sup>-1</sup> )	lnA (s <sup>-1</sup> )	S	R <sup>2</sup>
value	-35.7	35.4	296.87	38.97	0.01178	0.988

Kissinger methods, it can be inferred that the possible reaction model of the interaction reaction between Sb<sub>2</sub>S<sub>3</sub> and ZnO was inferred as R<sub>3</sub>. The corresponding values of the active energy and lnA are 275.3 kJ·mol<sup>-1</sup> and 31.6 s<sup>-1</sup>.

**Table 4.** Calculated results of kinetic parameters by Coats-Redfern method at heating rate of 10 K·min<sup>-1</sup>

No.	E (kJ·mol <sup>-1</sup> )	lnA (s <sup>-1</sup> )	S	R <sup>2</sup>
D <sub>1</sub>	411.8	53.3	10.37	0.783
D <sub>2</sub>	582.6	80	4.33	0.919
D <sub>3</sub>	563.6	75.7	7.07	0.909
A <sub>1.5</sub>	238.6	27.1	0.248	0.971
A <sub>2</sub>	175.8	17.2	0.14	0.97
A <sub>3</sub>	112.9	6.9	0.062	0.967
A <sub>4</sub>	81.48	1.7	0.035	0.965
R <sub>1</sub>	199.5	20.2	2.6	0.772
R <sub>2</sub>	250.3	27.9	2.173	0.864
R <sub>3</sub>	275.3	31.6	1.771	0.904
P <sub>2</sub>	93.3	3.3	0.652	0.747
P <sub>3</sub>	57.9	-2.6	0.29	0.718
P <sub>4</sub>	40.2	-5.6	0.164	0.685

Summary: the kinetic parameters of the roasting reactions between Sb<sub>2</sub>S<sub>3</sub> and ZnO were calculated by three different methods, and the average values of activation energy and the frequency factor by each method were showed in Table 5, and the average of these two parameters were also calculated in the table as 189.72 kJ·mol<sup>-1</sup> and 35.29 s<sup>-1</sup> respectively. According to the values of E and lnA, the kinetic equation of the roasting reaction can be obtained as shown in Eqs. (9).

**Table 5.** Average activation energy and frequency factor

Methods	Reaction	
	E (kJmol <sup>-1</sup> )	lnA (s <sup>-1</sup> )
Ozawa-Flynn-Wall	297	/
Kissinger	296.87	38.97
Coats-Redfern	275.3	31.6
Average	189.72	35.29

$$1-(1-\alpha)^{1/3} = 2.12 \times 10^{15} \exp\left(-\frac{1.90 \times 10^5}{RT}\right) t \quad (9)$$

#### 4. Conclusions

A new sulfur-fixed roasting method of Sb<sub>2</sub>S<sub>3</sub> by using ZnO as sulfur-fixed agent for stibnite extraction was proposed. The thermodynamics calculation and equilibrium dominance analysis indicated that the reaction process is completely feasible and easier to achieve with the temperature increase. The TG-DSC and XRD analyses showed that roasting reaction took place after 773 K and was basically completed at 873K. By using the method of TG-DSC, the non-isothermal kinetics of the roasting reaction between Sb<sub>2</sub>S<sub>3</sub> and ZnO was conducted to obtain the kinetics parameters. The average of activation energy and frequency factor calculated by Ozawa-Flynn-Wall, Kissinger and Coats-Redfern were 189.72 kJ·mol<sup>-1</sup> and 35.29 s<sup>-1</sup>, respectively. In addition, the results obtained by Ozawa-Flynn-Wall method showed that the mechanism of this reaction is phase boundary model (R<sub>3</sub>). The new method is expected to solve the shortcomings of low-concentration sulfur oxide emission and high energy consumption in the smelting of Sb<sub>2</sub>S<sub>3</sub>, as well as the comprehensive utilization of secondary ZnO material, and it also has a potential application in the extraction metallurgy of the congeneric sulfide ore.

#### Acknowledgements

This work was supported by the National Natural Science Foundation of China (No.51604105, No.51774127) and Foundation of Hunan Educational Committee (16C0463).

#### Reference

- [1] C.G. Anderson, *Chemie. der. Erde.*, 72 (2012) 3-8.
- [2] L.G. Ye, C.B. Tang, S.H. Yang, Y.M. Chen and W.H. Zhang, *J. Min. Metall. Sect. B-Metall.*, 51 (1) (2015) 97-103.
- [3] R. Padilla, A. Aracena and M.C. Ruiz, *J. Min. Metall. Sect. B-Metall.*, 50 (2) B (2014) 127-132.
- [4] R. Padilla, G. Ramirez and M.C. Ruiz, *Metall. Mater. Trans. B.*, 41B (2010) 1284-1292.
- [5] N. Štrbac, I. Mihajlović, D. Minić and Ž. Živković, *J. Min. Metall. Sect. B-Metall.*, 46 (1) B (2010) 75-86.
- [6] T.C. Zhao. *Antimony*. Beijing: Metallurgical Industry Press. 1978: 95.
- [7] T. Lei, C.W. Zhu and H.P. Zhang, *Antimony metallurgy*. Metallurgical Industry Press. 2009: 218-



- 235.
- [8] J.G. Yang, C.B. Tang, Y.M. Chen and M.T. Tang, Metall. Mater. Trans. B., 42 (2011) 30-36.
- [9] R.S. Multani, T. Feldmann and G.P. Demopoulos, Hydrometallurgy, 164 (2016) 141-153.
- [10] T. Mahlangu, F.P. Gudyanga and D.J. Simbi, Hydrometallurgy, 88 (2007) 132-142.
- [11] S. Steinlechner, J. Min. Metall. Sect. B-Metall., 54 (1) B (2018) 81-89.
- [12] S.A. Awe, J.E. Sundkvist, N.J. Bolin and Å. Sandström, Miner. Eng., 49 (2013) 45-53.
- [13] S.A. Awe and Å. Sandström, Miner. Eng., 23 (2010) 1227-1236.
- [14] J.G. Yang and Y.T. Wu, Hydrometallurgy, 143 (2014) 68-74.
- [15] W. Liu, H.L. Luo, W.Q. Qing and Y.X. Zheng, K. Yang and J.W. Han, Metall. Mater. Trans. B., 45 (4) (2014) 1281-1290.
- [16] Y.S. Meng, Y.X. Hua and F.L. Zhu, T. Indian. I. Metals, 68 (1) (2015) 37-41.
- [17] R. Padilla, L.C. Chambi and M.C. Ruiz, J. Min. Metall. Sect. B-Metall., 50 (1) (2014) 5-13.
- [18] L.G. Ye, C.B. Tang, Y.M. Chen, S.H. Yang, J.G. Yang and W.H. Zhang, J. Clean. Prod., 93 (2015) 134-139.
- [19] Z. Adamczyk and K. Nowińska, Environ. Earth Sci., 75(2016)1-6.
- [20] Y.X. Zheng, J.F. Lv, W. Liu, W.Q. Qin and S.M. Wen, Physicochem. Probl. Mi., 52(2016)943-954.
- [21] Y.X. Zheng, W. Liu, W.Q. Qin, K. Yang and H.L. Luo, Sep. Sci. Technol., 49(2014)783-791.
- [22] Y.X. Zheng, J.F. Lv, H. Wang, S.M. Wen and J. Pang, Sci. Rep-UK, 8(2018)1-10.
- [23] J.W. Han, W. Liu, T.F. Zhang, K. Xue, W.H. Li, F. Jiao and W.Q. Qin, Sci. Rep-UK, 7(2017)1-12.
- [24] J.F. Lv, X. Tong, Y.X. Zheng, X. Xie and C.B. Wang, Appl. Surf. Sci., 437(2018)13-18.
- [25] L. Xiao, L. Li, F. Fu and M. He, Thermochim. Acta, 541 (2012) 57-61.
- [26] B. Boonchom and S. Puttawong, Physica. B 405 (2010) 2350-2355.
- [27] L.H. He, X.H. Liu and Z.W. Zhao, Thermochim. Acta, 566 (2013) 298-304.
- [28] K. Jayaraman, M. V. Kok and I. Gokalp, Renew Energ., 101 (2017) 293-300.
- [29] Z. Ouyang, S.F. Liu, C.B. Tang, Y.F. Chen and L.G. Ye, Vacuum, 159 (2019)358-366.
- [30] W.Q. Qin, H.L. Luo, W. Liu and Y.X. Zheng, K. Yang and J.W. Han, J. Cent. South Univ., 22 (3) (2015) 868-873.

## TERMODINAMIČKA I KINETIČKA ANALIZA PRŽENJA SULFIDA ANTIMONA KORIŠĆENJEM ZnO KAO AGENSA ZA FIKSIRANJE SUMPORA

Z. Ouyang<sup>a</sup>, Y.F. Chen<sup>a</sup>, S.Y. Tian<sup>a</sup>, L. Xiao<sup>a</sup>, C.B. Tang<sup>b</sup>, Y. J. Hu<sup>a</sup>, Z. M. Xia<sup>a</sup>, Y.M. Chen<sup>b</sup>, L.G. Ye<sup>a\*</sup>

<sup>a\*</sup>Fakultet za metalurgiju i inženjerstvo materijala, Univerzitet za tehnologiju u Hunanu, Džudžou, Kina

<sup>b</sup>Fakultet za metalurgiju i zaštitu životne sredine, Centralno-južni univerzitet, Čangša, Kina.

### Apstrakt

Komercijalna metalurgija antimona je trenutno zasnovana na pirometalurškim procesima, i oksidativno isparavanje Sb<sub>2</sub>S<sub>3</sub> je neophodan korak koji sa sobom nosi probleme velike potrošnje energije i niske koncentracije SO<sub>2</sub> zagađenja. U cilju rešenja ovih problema predstavljen je novi metod prženja sulfida antimona gde se fiksira sumpor. Ovaj metod koristi ZnO kao agens za fiksiranje sumpora, i prženje sa Sb<sub>2</sub>S<sub>3</sub> je izvedeno na temperaturi od 673 K~1073 K da bi se dobio Sb<sub>2</sub>O<sub>3</sub> i ZnS. Termodinamičkom analizom reakcija možemo zaključiti da je promena Gibsove slobodne energije ( $\Delta G^0$ ) reakcije prženja ispod -60 kJ/mol, a da su predominantne oblasti Sb<sub>2</sub>O<sub>3</sub> i ZnS široke i da se sa porastom temperature pomeraju udesno, što sve ukazuje na to da je ovaj metod teoretski izvodljiv. Produkti reakcije između Sb<sub>2</sub>S<sub>3</sub> i ZnO ukazuju na to da je reakcija počela na 773 K i završila se približno na 973K. Koristili smo Ozawa-Flynn-Wall, Kissinger i Coats-Redfern metod za izračunavanje kinetike reakcije prženja. Zaključak je sledeći: prosečne vrednosti aktivacione energije (E) i prirodnog logaritamskog faktora frekvencije (lnA) izračunate uz pomoć Ozawa-Flynn-Wall, Kissinger i Coats-Redfern metoda bile su 189.72 kJ·mol<sup>-1</sup> i 35.29 s<sup>-1</sup>. Mehanizam ove reakcije je bio model reakcije granične faze. Kinetički model je prikazan jednačinom:

$$1-(1-\alpha)^{1/3} = 2.12 \times 10^{15} \exp\left(-\frac{1.90 \times 10^5}{RT}\right)t$$

gde  $\alpha$  predstavlja stepen izreagovanosti.

**Cljučne reči:** Sulfid antimona; Cink oksid; Fiksiranje sumpora; Kinetika; Prženje

